

Supplementary Information

for

**Two- and three-body fragmentation of multiply charged tribromomethane by
ultrafast laser pulses†**

Authors: Surjendu Bhattacharyya,^a Kurtis Borne,^a Farzaneh Ziaee,^a Shashank Pathak,^a Enliang Wang,^{a,b} Anbu Selvam Venkatachalam,^a Nathan Marshall,^a Kevin D. Carnes,^a Charles W. Fehrenbach,^a Travis Severt,^a Itzik Ben-Itzhak,^a Artem Rudenko^a and Daniel Rolles^{*a}

^a J. R. Macdonald Laboratory, Department of Physics, Kansas State University,
Manhattan, KS 66506, USA. E-mail: rolles@phys.ksu.

^bHefei National Laboratory for Physical Sciences at the Microscale and Department of Modern Physics,
University of Science and Technology of China, Hefei 230026, China.

Figures

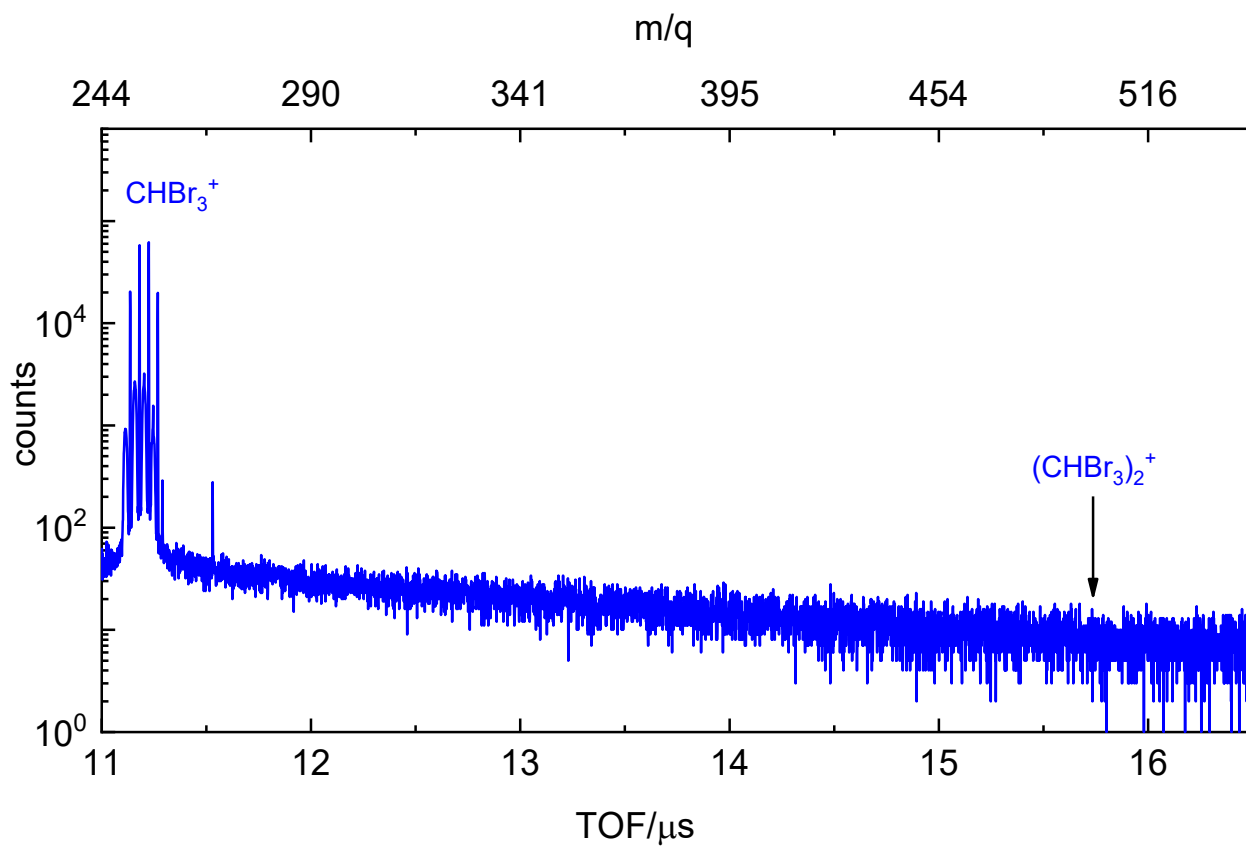
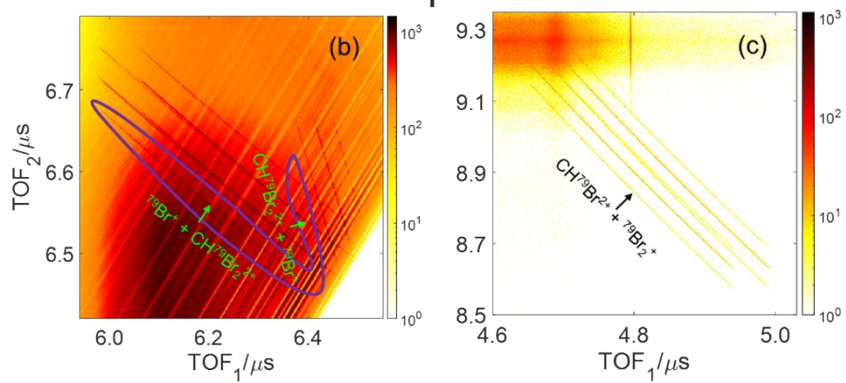
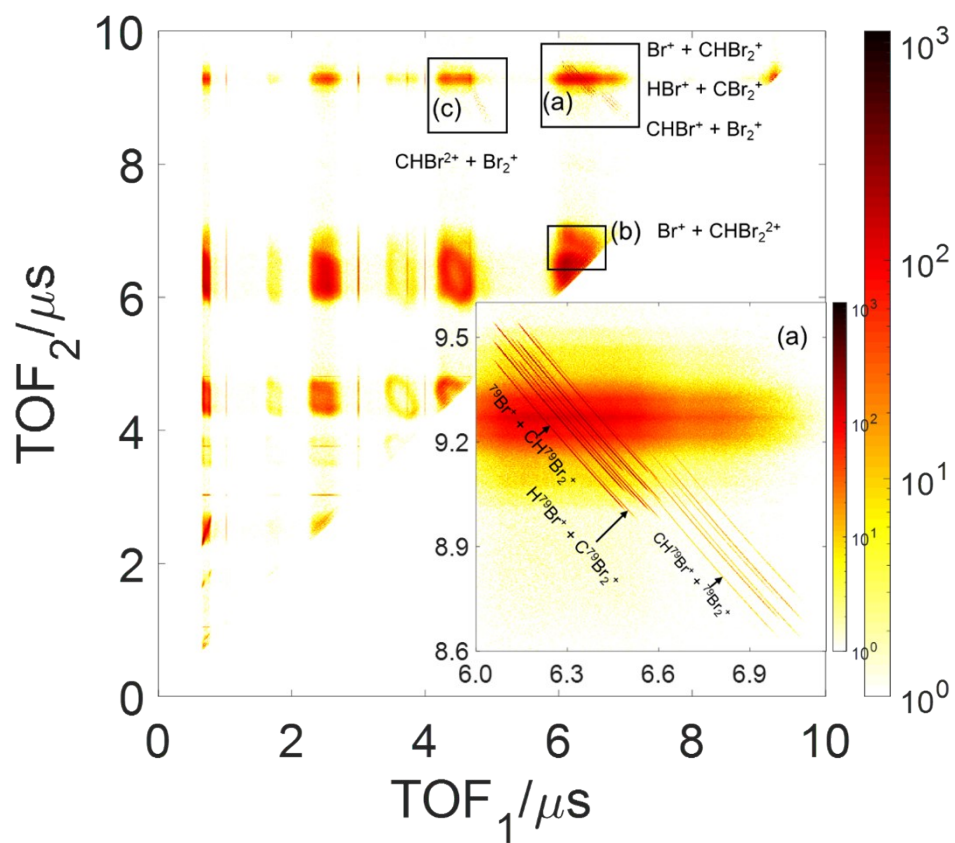


Fig. S1 Selected region of the time-of-flight (TOF) mass spectrum (m/q is shown on the top) of CHBr_3 to indicate the position of the $(\text{CHBr}_3)_2^+$ dimer ion under the same conditions as Fig. 2. There is no evidence of cluster formation.



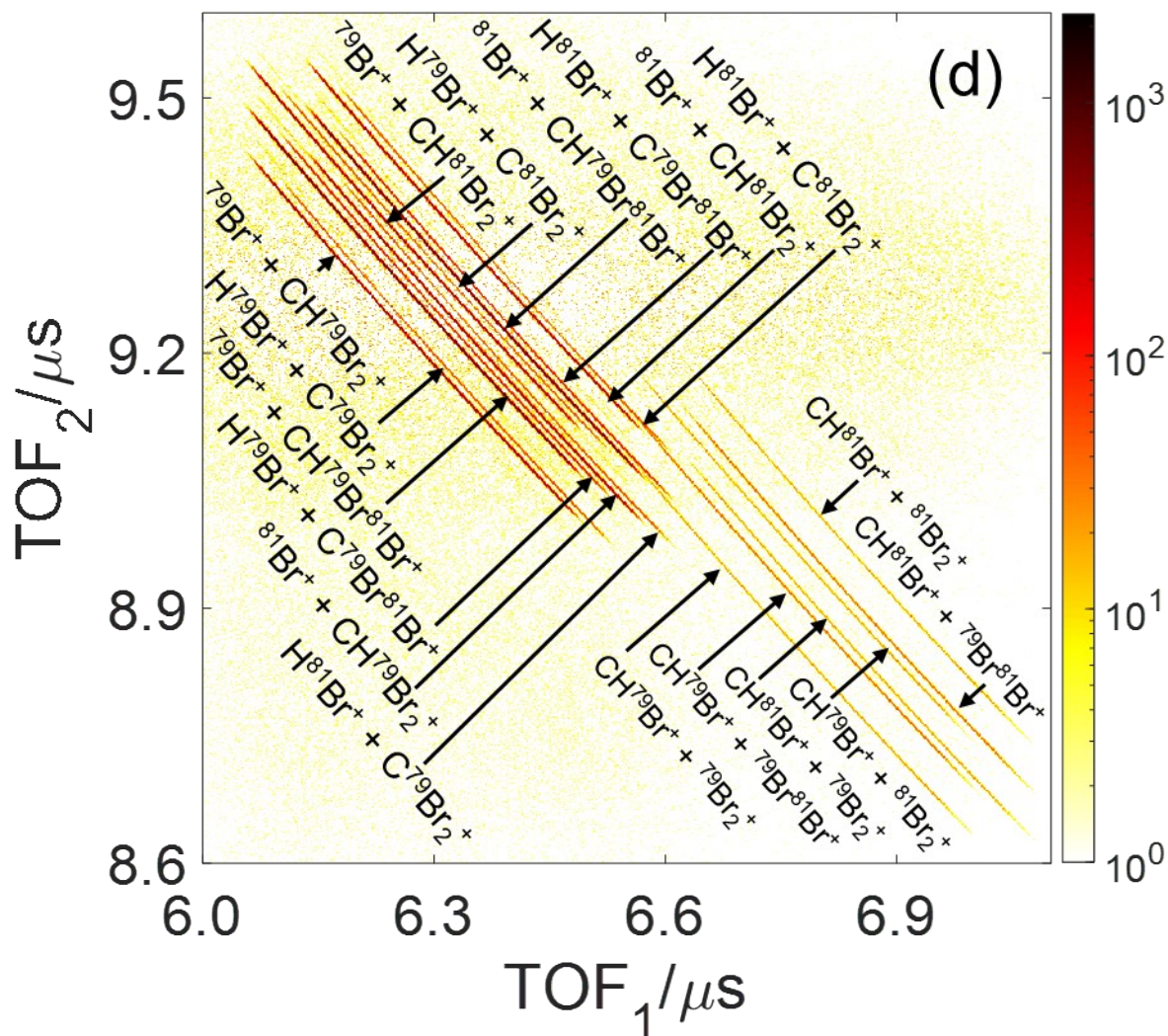


Fig. S2 PhotoIon–PhotoIon COincidence (PIPICO) plot of CHBr_3 for the same conditions as Fig. S1 *without* subtraction of random coincidences. The ion yield is plotted as a function of the time of flight of the first and second detected ions. The dominant channels appear in the region marked by the black square as diagonal stripes. This region is shown again in the inset. The black squares labeled (a), (b) and (c) indicate the regions of interest where the five main channels $\text{Br}^+ + \text{CHBr}_2^+$, $\text{HBr}^+ + \text{CBr}_2^+$, $\text{CHBr}^+ + \text{Br}_2^+$, $\text{CHBr}^{2+} + \text{Br}_2^+$, and $\text{Br}^+ + \text{CHBr}_2^+$ appear. (d) Detailed assignment of region (a) after random subtraction. The broad “island” features in this plot are due to breakup into more than three fragments as well as a significant amount of random (false) coincidences because of the fairly high-count rate in our experiment (20 kHz ion counts at a 10 kHz laser repetition rate).

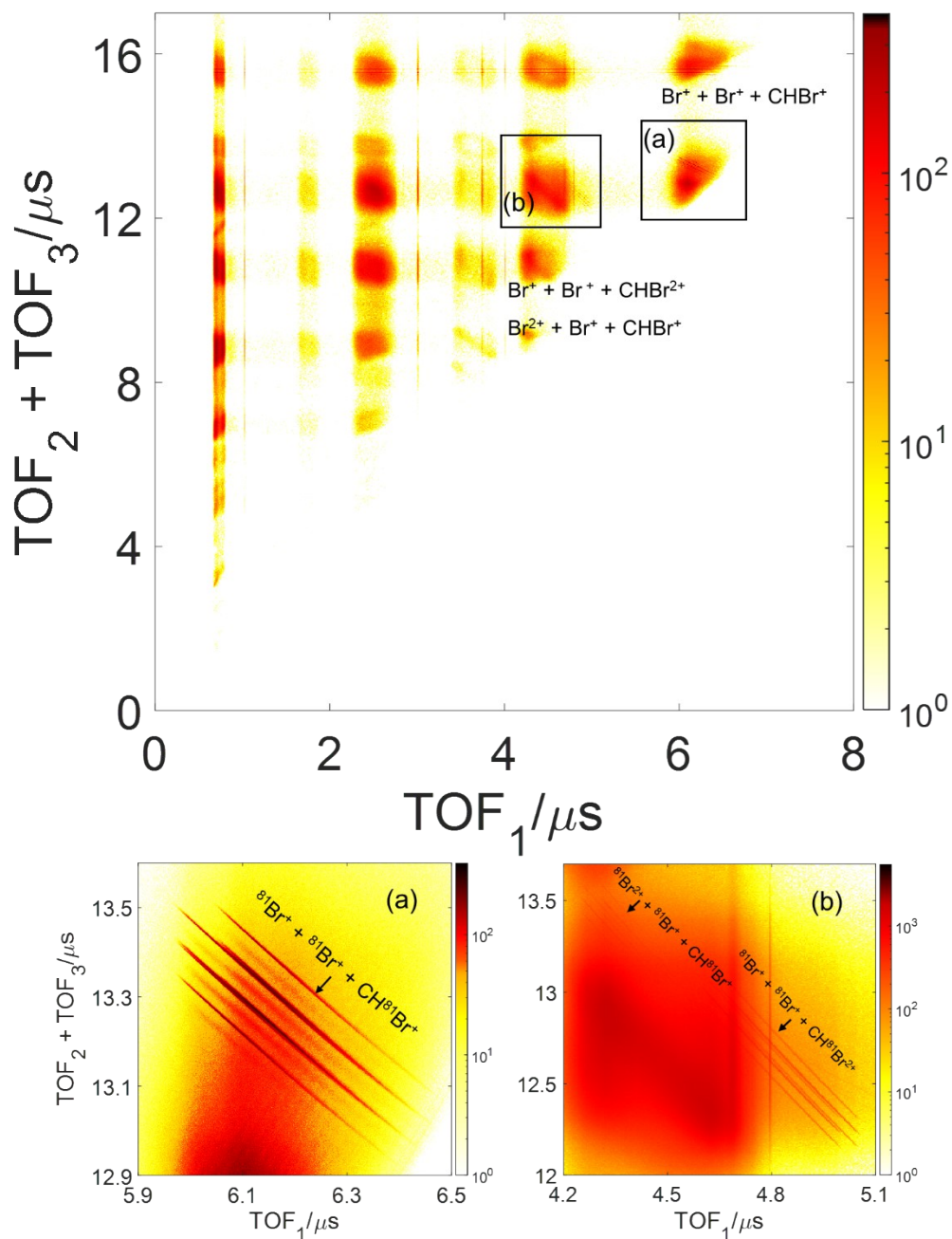


Fig. S3 TRIPICO plot of CHBr_3 . The ion yield is plotted as a function of the time of flight of the first and the sum of times of flight of the second and third detected ions. The dominant channels appear in the regions marked by the black squares as diagonal stripes. These regions are shown again in the bottom panels. The black squares labeled (a) and (b) indicate the regions of interest where the three main channels $\text{Br}^+ + \text{Br}^+ + \text{CHBr}^+$, $\text{CHBr}^{2+} + \text{Br}^+ + \text{Br}^+$ and $\text{Br}^{2+} + \text{Br}^+ + \text{CHBr}^+$ appear. Multiple diagonal stripes are due to the possible combinations of the two naturally occurring isotopes of Br (^{79}Br and ^{81}Br).

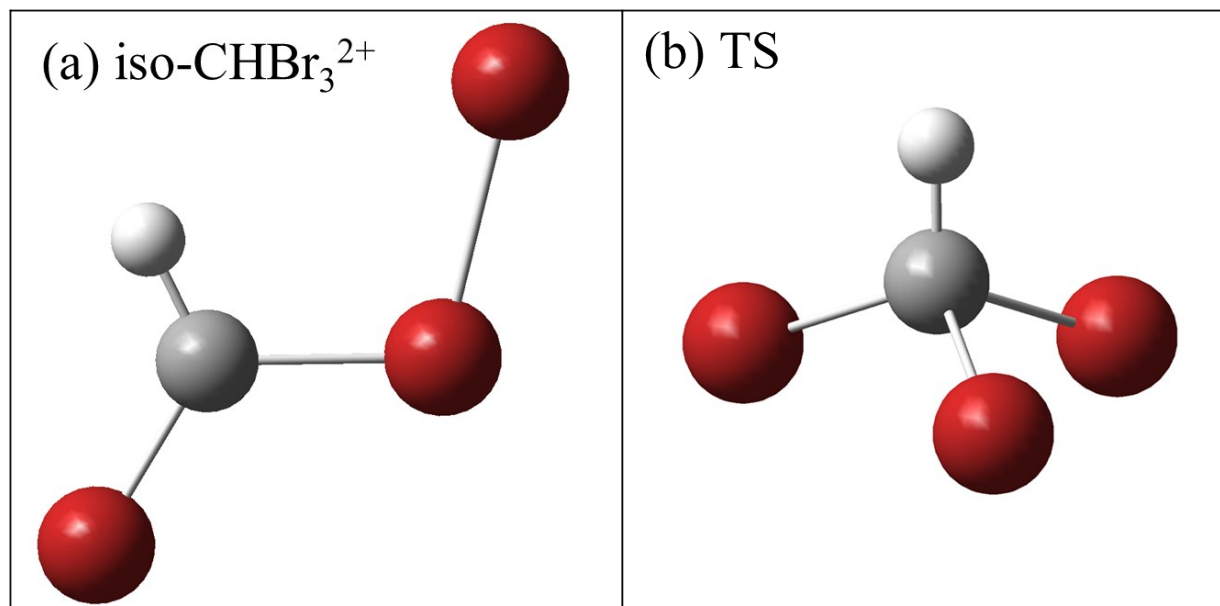


Fig. S4 Optimized structures of the (a) $\text{BrHCBBr}-\text{Br}^{2+}$ isomer (iso-CHBr_3^{2+}) and (b) transition state (TS) structure correlated to vertically ionized CHBr_3^{2+} and iso-CHBr_3^{2+} . Both structures are calculated at the $\omega\text{B97x-d/aug-cc-pVDZ}$ level of theory on the singlet ground state of the dication. The transition state has only a single imaginary frequency with a negative eigenvalue of the Hessian, thus ensuring that it is a true local minimum. Intrinsic reaction coordinate (IRC) calculations show that the reaction path from TS ends in a chemically bonded structure closely resembling iso-CHBr_3^{2+} but with an H-C-Br-Br dihedral angle of 70° . The electronic energies of iso-CHBr_3^{2+} and TS are 25.3 and 27.1 eV, respectively, with respect to the electronic energy of neutral CHBr_3 .

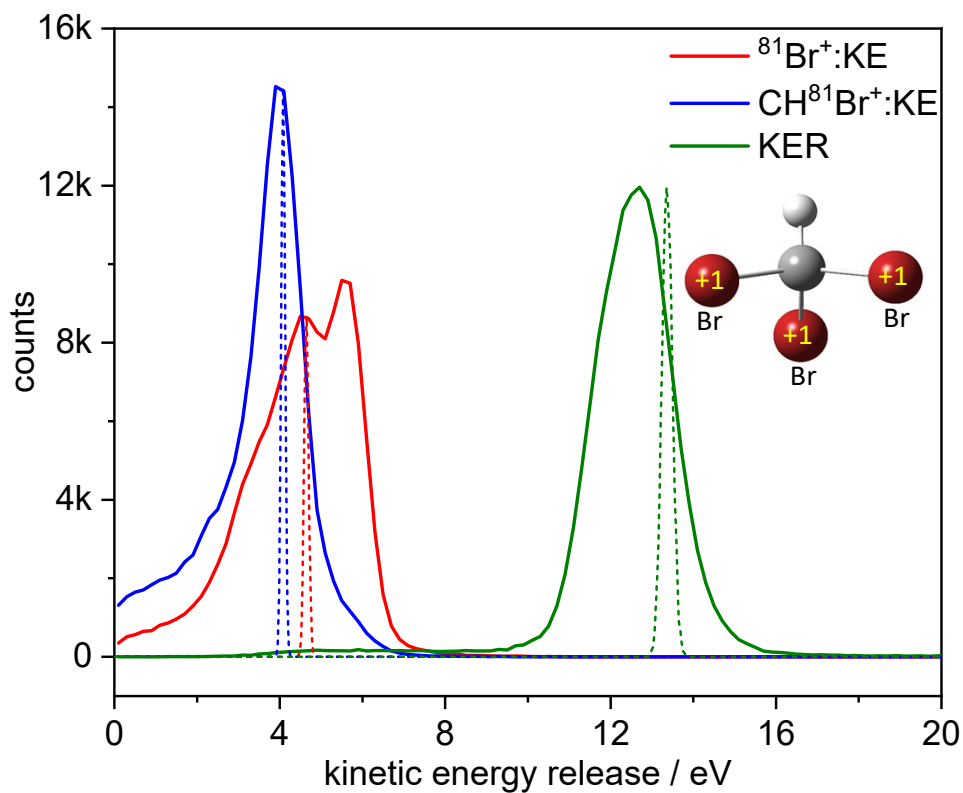


Fig. S5 Comparison of the measured ion kinetic energy release distributions (solid lines) for three-body fragmentation of CHBr_3 into $^{81}\text{Br}^+ + ^{81}\text{Br}^+ + \text{CH}^{81}\text{Br}^+$, as shown in Fig. 8, with the Coulomb explosion simulations (dashed lines) for the three-body fragmentation of ten thousand CHBr_3 geometries sampling the Wigner distribution of the ground-state molecules at 60 K. The simulated distributions are normalized with the peak height of the respective measured distributions.